ARTICLE IN PRESS

Kuwait Journal of Science xxx (xxxx) xxx

Contents lists available at ScienceDirect

Kuwait Journal of Science

journal homepage: www.sciencedirect.com/journal/kuwait-journal-of-science

Full length article

Numerical treatments of nonlinear Burgers–Fisher equation via a combined approximation technique

Mohammad Izadi [a,*], Hari Mohan Srivastava [b,c,d,e]

[a] Department of Applied Mathematics, Faculty of Mathematics and Computer, Shahid Bahonar University of Kerman, Kerman, Iran
[b] Department of Mathematics and Statistics, University of Victoria, Victoria, British Columbia V8W 3R4, Canada
[c] Department of Medical Research, China Medical University Hospital, China Medical University, Taichung 40402, Taiwan
[d] Department of Mathematics and Informatics, Azerbaijan University, 71 Jeyhun Hajibeyli Street, AZ1007 Baku, Azerbaijan
[e] Center for Converging Humanities, Kyung Hee University, 26 Kyungheedae-ro, Dongdaemun-gu, Seoul 02447, Republic of Korea

ARTICLE INFO

MSC:
26A33
65L60
42C05
65L05

Keywords:
Boole polynomials
Burgers–Fisher equation
Convergence analysis
Collocation points
Taylor expansion

ABSTRACT

A combined spectral matrix collocation strategy is presented to solve the time-dependent nonlinear Burgers–Fisher equation pertaining to various important physical mechanisms such as advection, diffusion, and logistic reaction. The nonlinearity of the model is first tackled by a time-marching scheme based on the Taylor formula. Hence in each time step, we solve a linear initial boundary value problem (IBVP) by using the spectral collocation technique based on novel Boole polynomials. Various numerical computations are carried out to indicate the pertinent features and testify the applicability of the presented combined technique. Comparisons are made between our results and the exact analytical solutions and some available numerical outcomes in the literature to show the validity of the method.

Introduction

The modeling of real-world physical phenomena and natural complex systems has been always an active area of ongoing interest for the research community. Mathematical modeling of many of such events usually leads to nonlinear partial differential equations (PDEs). The nonlinear Burgers–Fisher model as a mixed hyperbolic–parabolic PDE can be used to describe the interaction between various mechanism such as nonlinear logistic reaction, linear diffusion or nonlinear advection effects. The fundamental goal of this manuscript is to present an efficient computational procedure to find the solutions of the nonlinear Burgers–Fisher equation

$$\frac{\partial w}{\partial t} + \alpha\, w\, \frac{\partial w}{\partial x} + \beta\, w\,(1-w) = \gamma\, \frac{\partial^2 w}{\partial x^2}, \quad 0 \le x \le 1,\ 0 \le t \le T, \tag{1}$$

where $T > 0$ is a given final time, $\alpha \in \mathbb{R}$ denotes the advection constant, $\beta \le 0$ is the source or sink constant, and $\gamma > 0$ denotes the diffusion coefficient. The model equation (1) is subjected to the initial condition

$$w(x, t = 0) = w_0(x), \quad 0 \le x \le 1, \tag{2}$$

and the given boundary conditions are as follow

$$w(x = 0, t) = f_0(t), \qquad w(x = 1, t) = f_1(t), \quad 0 \le t \le T, \tag{3}$$

where $f_0(t)$ and $f_1(t)$ are two prescribed functions. So far, diverse approximation algorithms have been provided for the numerical treatments of Burgers–Fisher equation. For instance, let us mention the Tanh method (Wazwaz, 2005), the compact finite difference technique (Sari et al., 2010), the finite difference methods (FDMs) (Chandrakera et al., 2015; Izadi and Srivastava, 2022; Roul and Rohil, 2022; Izadi, 2021), the homotopy perturbation method (Rashidi et al., 2009), the local discontinuous GalerkinI method (Zhang et al., 2012), the optimal homotopy asymptotic scheme (Nawaz et al., 2013), the analytic exp-function approach (Malik et al., 2015), the enhanced modified simple equation strategy (Zhang and Zhang, 2017), the B-spline collocation method (Singh et al., 2020), the finite element methods (Yadav and Jiwari, 2017; Izadi, 2020), and the nonstandard finite difference scheme (Namjoo et al., 2018). Some more analytical as well as computational approaches to solve different closely related model equations to (1) such as the simultaneously compact FDMs for (general) PDEs (Doostaki et al., 2023), the hybrid computational procedures for Burgers and convection–diffusion (CD) equations (Jiwari, 2015; Negero and Duressa, 2022), the two-stages explicit FDMs and the Rothe–Newton spectral method for CD problems (Izadi, 2022; Srivastava and Izadi, 2022), the meshless procedures based on global

* Corresponding author.
E-mail addresses: izadi@uk.ac.ir (M. Izadi), harimsri@math.uvic.ca (H.M. Srivastava).

https://doi.org/10.1016/j.kjs.2023.12.003
Received 12 September 2023; Received in revised form 4 December 2023; Accepted 7 December 2023
Available online 9 December 2023

Please cite this article as: Mohammad Izadi, Hari Mohan Srivastava, *Kuwait Journal of Science*, https://doi.org/10.1016/j.kjs.2023.12.003

and local radial basis functions to simulate the behavior of Burgers' type and reaction–diffusion (RD) model problems (Jiwari et al., 2019; Jiwari, 2022; Jiwari and Gerisch, 2021), the traveling wave transformation for 2D Burgers-type models (Yang et al., 2017), the Lie group analysis for Boussinesq–Burgers equations (Bira et al., 2019), the FD-based procedure for the novel RD covid-19 model (Ahmed et al., 2021), the predictor–corrector approach for discontinuous conservation laws (Okhovati and Izadi, 2020), and the reduced differential transform algorithm for $(1+n)$-D Burgers equations (Srivastava et al., 2014).

The chief goal of the current research work is to examine a novel combined approximative strategy for the unsteady and nonlinear Burgers–Fisher equation. The inherent nonlinearity together with time dependency of the model makes it difficult to devise an accurate as well as efficient numerical approach for it. On the other hand, most of time-marching algorithms allow only a small time step size so that the overall computational complexity of the algorithm becomes too high. This limiting factors motivate us to design a novel combined procedure to solve the nonlinear model equation (1). In this work, we employ the Taylor formula as a time-marching procedure which allows us to tackle the nonlinearity of the model and is capable of giving high accurate results (with second-order accuracy in time) compared to existing well-established numerical methods.

Spectral based collocation techniques are promising in obtaining the approximate solutions of such model problems accurately and with exponential convergence. In the space variable, a spectral matrix technique using the (novel) Boole functions are employed to approximate the solutions of the discretized time equations. This set of functions considered in the previous works (Jordan, 1950; Roman, 1984; Kim and Kim, 2014; Simsek and So, 2019; Bicer and Dag, 2023). Furthermore, the exponential convergence properties of these Boole functions are established in this study for the first time to the best of our knowledge. The benefits of spectral collocation methodologies by using various polynomials have been tested previously through several research papers. To review, let us mention some of them like the collocations strategies based on the Bessel (Izadi et al., 2023; Izadi and Srivastava, 2023), Chebyshev (Razavi et al., 2022; Khader and Saad, 2018), airfoil (Srivastava and Izadi, 2023), Bernstein Ahmed (2019), Vieta–Fibonacci (Izadi and Roul, 2023), Lagrange (Sabermahani et al., 2021), and Jacobi polynomials (Youssri and Hafez, 2019).

The organization of the present manuscript is provided next. A concise review of the novel Boole polynomials is described in Section "The Boole polynomials". A detailed consideration of temporal discretization for the Burger–Fisher equation is performed in Section "Temporal discretization". A convergence study of the Boole functions is established in a rigorous way in Section "Main matrix relations of Boole polynomials and their convergence results". The illustrations of the combined Taylor–Boole scheme is carried out in Section "The combined collocation method". A justification of the proposed combined approach is accomplished through simulating several numerical experiments in Section "Experimental results and discussions". A conclusion finally is drawn in Section "Experimental results and discussions".

The Boole polynomials

Jordan (1950) was the first one to use a series of Boole polynomials for the formal expansion of a given function. These polynomials are also important in many disciplines such as umbral calculus (Roman, 1984) and number theory (Kim and Kim, 2014)

These sequence of polynomials are defined explicitly by

$$\mathrm{B}_q(x)=\sum_{k=0}^{q}\frac{(-1)^k}{2^k}\binom{x}{q-k},\quad q=0,1,\dots, \tag{4}$$

where we have used the notations

$$\binom{x}{s}:=\frac{x(x-1)(x-2)\dots(x-s+1)}{s!},\quad \binom{x}{0}:=1,\quad \binom{x}{1}:=1.$$

This implies that $\mathrm{B}_0(x)=1$ and $\mathrm{B}_1(x)=-\frac{1}{2}+x$. The list of next Boole polynomials of degrees 2 to 5 are given as

$$\begin{aligned}
\mathrm{B}_2(x)&=\frac{1}{4}-x+\frac{1}{2}x^2,\\
\mathrm{B}_3(x)&=-\frac{1}{8}+\frac{5}{6}x-\frac{3}{4}x^2+\frac{1}{6}x^3,\\
\mathrm{B}_4(x)&=\frac{1}{16}-\frac{2}{3}x+\frac{5}{6}x^2-\frac{1}{3}x^3+\frac{1}{24}x^4,\\
\mathrm{B}_5(x)&=-\frac{1}{32}+\frac{8}{15}x-\frac{5}{6}x^2+\frac{11}{24}x^3-\frac{5}{48}x^4+\frac{1}{120}x^5.
\end{aligned}$$

In fact, these polynomials are related to another parameter $\lambda\neq 0$ as discussed in Roman (1984). The generating function for this set is given by

$$\sum_{q=0}^{\infty}\frac{\mathrm{B}_q(x)}{q!}t^q=(1+t)^x\left[(1+t)^\lambda+1\right]^{-1}.$$

For $x=0$ we derive the so-called the Boole numbers (Kim and Kim, 2014) associated to the Boole polynomials. One can easily seen that $B_q(0)=\frac{(-1)^q}{2^q}$.

Below, we use the vector of Boole polynomials of size $\mathcal{N}$, where $\mathcal{N}$ is a positive integer. Denote this aforementioned vector as $\boldsymbol{B}_{\mathcal{N}}$, which is defined by

$$\boldsymbol{B}_{\mathcal{N}}(x)=\left[\mathrm{B}_0(x)\quad \mathrm{B}_1(x)\quad \dots\quad \mathrm{B}_{\mathcal{N}}(x)\right].$$

To proceed, we define the vector of monomial basis functions

$$\boldsymbol{X}_{\mathcal{N}}(x)=\left[1\quad x\quad x^2\quad \dots\quad x^{\mathcal{N}}\right]. \tag{5}$$

From the above discussions on these polynomials and according to the expansion series (4) one can show that

$$\boldsymbol{B}_{\mathcal{N}}(x):=\boldsymbol{X}_{\mathcal{N}}(x)\,\boldsymbol{D}^t. \tag{6}$$

Here, the matrix $\boldsymbol{D}$ has a lower-triangular structure. For instance, if we take $\mathcal{N}=5$, we get the following matrix of size 6×6 as

$$\boldsymbol{D}^t:=\begin{pmatrix}
\frac{1}{0!} & -\frac{1}{2} & \frac{1}{4} & -\frac{1}{8} & \frac{1}{16} & -\frac{1}{32}\\
0 & \frac{1}{1!} & -1 & \frac{5}{6} & -\frac{2}{3} & \frac{8}{15}\\
0 & 0 & \frac{1}{2!} & -\frac{3}{4} & \frac{5}{6} & -\frac{5}{6}\\
0 & 0 & 0 & \frac{1}{3!} & -\frac{1}{3} & \frac{11}{24}\\
0 & 0 & 0 & 0 & \frac{1}{4!} & -\frac{5}{48}\\
0 & 0 & 0 & 0 & 0 & \frac{1}{5!}
\end{pmatrix}_{6\times 6}.$$

Furthermore, it can be shown that derivative of the monomial vector $\boldsymbol{X}_{\mathcal{N}}(x)$ in (5) can be stated as

$$\frac{d}{dx}\boldsymbol{X}_{\mathcal{N}}(x)=\boldsymbol{X}_{\mathcal{N}}(x)\boldsymbol{Q}^t,\quad \boldsymbol{Q}^t=\begin{pmatrix}
0 & 1 & 0 & \dots & 0\\
0 & 0 & 2 & \dots & 0\\
\vdots & \vdots & \ddots & \vdots & \vdots\\
0 & 0 & 0 & \ddots & \mathcal{N}\\
0 & 0 & 0 & \dots & 0
\end{pmatrix}_{(\mathcal{N}+1)\times(\mathcal{N}+1)}. \tag{7}$$

Temporal discretization

Let us first discretize the Burgers–Fisher equation in time. To this end, a division of $[0,T]$ into $\mathcal{M}$ equal pieces will be considered such that the nodes are

$$t_0=0<t_1=\delta t<\dots<t_{\mathcal{M}}=\mathcal{M}\delta t=T.$$

Here, the (uniform) time-step is $\delta t=t_n-t_{n-1}$ for $n=1,2,\dots,\mathcal{M}$. In order to have a higher-order accuracy with regard to the time variable, we consider the Taylor expansion formula for the function $w^n(x)=w(x,t_n)$ as

$$w_t^n=\frac{w^{n+1}-w^n}{\delta t}-\frac{1}{2}\delta t\, w_{tt}^n+\mathcal{O}(\delta t^2). \tag{8}$$

By differentiating (1) with regard to t, we arrive at

$$w_{tt}^n = \left[\gamma\, w_{xx}^n - \alpha\, w^n\, w_x^n - \beta\, w^n\,(1-w^n)\right]_t$$
$$= \gamma\, w_{xxt}^n - \alpha\, w_t^n\, w_x^n - \alpha\, w^n\, w_{xt}^n - \beta\, w_t^n + 2\beta\, w^n\, w_t^n.$$

We now substitute the first order derivatives w_t^n in all occurrences by $\frac{w^{n+1}-w^n}{\delta t}$. Thus, we may write w_{tt}^n as

$$\delta t\, w_{tt}^n = \gamma(w_{xx}^{n+1} - w_{xx}^n) - \alpha\, w^n(w_x^{n+1} - w_x^n) - \left[\alpha\, w_x^n + \beta(1-2w^n)\right](w^{n+1} - w^n). \tag{9}$$

We next put (9) into the right part of (8) and utilize the time discretized form of (1), namely

$$w_t^n = \gamma\, w_{xx}^n - \alpha\, w^n\, w_x^n - \beta\, w^n\,(1-w^n),$$

in the left-hand side of (8). The discretized equation of time for (1) of order $\mathcal{O}(\delta t^2)$ is now available after some modifications

$$\left[2 + \delta t\Big(\alpha\, w_x^n + \beta(1-2w^n)\Big)\right] w^{n+1} + \alpha\delta t\, w^n\, w_x^{n+1} - \delta t\, \gamma\, w_{xx}^{n+1} = 2w^n + \delta t(\gamma\, w_{xx}^n - \beta\, w^n), \tag{10}$$

for $n = 0, 1, \ldots, \mathcal{M}-1$. To begin calculations with (10), we require $w^0 = w_0(x)$ and its first and second-order derivatives. Obviously, $w_0(x)$ is obtained from the initial condition (2). On the other hand, at $x = 0, 1$, we also prescribe the next boundary conditions in accordance to (3) as

$$w^{n+1}(0) := f_0^{n+1} = f_0(t_{n+1}), \quad w^{n+1}(1) := f_1^{n+1} = f_1(t_{n+1}), \quad n = 0, 1, \ldots, \mathcal{M}-1. \tag{11}$$

Main matrix relations of Boole polynomials and their convergence results

Once the Burgers–Fisher equation is discretized in time via relation (10), the next step is to find the approximate solution in the space variable x. Towards this end, the linear second-order boundary-value problems (10)–(11) will be solved. We look for the solutions w^{n+1} in terms of Boole functions (4) in each time level. The values $w^0(x)$ at $n = 0$ is obtained from the given initial condition $w_0(x)$. Let us by $\mathcal{V}_{n,\mathcal{N}}(x)$ we denote the computed Boole approximation to w^n at t_n. Now, we seek the new approximation $\mathcal{V}_{n+1,\mathcal{N}}(x)$ at the next time-step t_{n+1} $(n = 0, 1, \ldots, \mathcal{M}-1)$ as

$$\mathcal{V}_{n+1,\mathcal{N}}(x) = \sum_{q=0}^{\mathcal{N}} a_q^n\, \mathrm{B}_q(x), \quad x \in [0,1], \tag{12}$$

with a_q^n, $0 \le q \le \mathcal{N}$ as the unknowns coefficient related to Boole functions have to be found. In the matrix form, the cutted Boole series (12) is written as

$$\mathcal{V}_{n+1,\mathcal{N}}(x) = \boldsymbol{B}_{\mathcal{N}}(x)\, \boldsymbol{A}_{\mathcal{N}}^n. \tag{13}$$

In (13), $\boldsymbol{A}_{\mathcal{N}}^n$ being the unknown vector given by

$$\boldsymbol{A}_{\mathcal{N}}^n = \begin{bmatrix} a_0^n & a_1^n & \ldots & a_{\mathcal{N}}^n \end{bmatrix}^t,$$

and $\boldsymbol{B}_{\mathcal{N}}(x)$ is the vector of Boole functions given in (6).

Next, we examine the L_2-convergence study of the Boole bases on $[0,1]$. Let us suppose that g_1 and g_2 are two real-valued functions. The associated inner product with respect to $\omega(x) \equiv 1$ and its induced norm are given by

$$(g_1, g_2)_\omega := \int_0^1 g_1(x)\, g_2(x)\, \omega(x) dx, \quad \text{and} \quad \|g_1\|_\omega^2 = (g_1, g_1)_\omega.$$

The corresponding space of functions is also defined by

$$\mathcal{L}_{\omega,2}([0,1]) := \{y : [0,1] \to \mathbb{R} \;:\; y \text{ is measurable and } \|y\|_\omega < \infty\}.$$

We then consider a finite dimensional space $\mathbb{W}_{\mathcal{N}} \subseteq \mathcal{L}_{\omega,2}$ spanned by the Boole bases given by

$$\mathbb{W}_{\mathcal{N}} = \mathrm{Span}\langle \mathrm{B}_0(x), \mathrm{B}_1(x), \ldots, \mathrm{B}_{\mathcal{N}}(x)\rangle.$$

It is evident that the space $\mathbb{W}_{\mathcal{N}}$ is of finite dimensional and consequently a closed subspace of $\mathcal{L}_{\omega,2}$. From approximation theory we know that $\mathbb{W}_{\mathcal{N}}$ is a complete subspace of $\mathcal{L}_{\omega,2}$. Now, the existence of a member $f^*(x) \in \mathcal{L}_{\omega,2}([0,1])$ as the best (closet) approximations to the elements of $\mathbb{W}_{\mathcal{N}}$ is guaranteed. Mathematically, it implies that

$$\|f - f^*\|_\omega \le \|f - g\|_\omega, \tag{14}$$

for all $g \in \mathbb{W}_{\mathcal{N}}$.

A result from approximation theory (Stewart, 1996) is mentioned next.

Theorem 1. *Suppose that $f \in C^{\mathcal{N}}([0,1])$ and $P_{\mathcal{N}}(x)$ shows the associated interpolating function of f at $\mathcal{N}$ Chebyshev zeros (nodes) on $[0,1]$. Thus, the following upper bound is valid*

$$|f(x) - P_{\mathcal{N}}(x)| \le \frac{2\|f\|_\infty}{4^{\mathcal{N}}\,\mathcal{N}!}, \quad \|f\|_\infty := \max_{\eta\in[0,1]} |f^{(\mathcal{N})}(\eta)|.$$

We will now establish and demonstrate the convergence result for the Boole expansion series in the $\mathcal{L}_{\omega,2}$ weighted space.

Theorem 2. *Let suppose that $f \in C^{(\mathcal{N}+1)}[0,1] \cap \mathcal{L}_{\omega,2}[0,1]$. Suppose also $f_{\mathcal{N}}(x) = \boldsymbol{B}_{\mathcal{N}}(x)\,\boldsymbol{A}_{\mathcal{N}}^n$ be the finest approximation of $f(x)$ out of $\mathbb{W}_{\mathcal{N}}$ at time level t_n. Denoting $E_{\mathcal{N}}(x) := f(x) - f_{\mathcal{N}}(x)$, we have*

$$\|E_{\mathcal{N}}\|_\omega \le \frac{\|f\|_\infty}{4^{\mathcal{N}}\,(\mathcal{N}+1)!}.$$

Proof. By utilizing Theorem 1 to the given function $f(x)$ with $(\mathcal{N}+1)$ Chebyshev nodes we get the following error bound

$$|f(x) - P_{\mathcal{N}+1}(x)| \le \frac{2\|f\|_\infty}{(\mathcal{N}+1)!\,4^{\mathcal{N}+1}}, \quad x \in [0,1].$$

On account of given assumptions of the theorem, the approximation $f_{\mathcal{N}}(x)$ shows the closet approximation in the space $\mathbb{W}_{\mathcal{N}}$. The immediate conclusion by the relation (14) is

$$E_{\mathcal{N}}(x) \le \|f(x) - g(x)\|_\omega, \quad \forall g \in \mathbb{W}_{\mathcal{N}}.$$

Especially for $g = P_{\mathcal{N}+1}(x) \in \mathbb{W}_{\mathcal{N}}$ in the last relation we conclude that

$$E_{\mathcal{N}}^2(x) \le \|f(x) - P_{\mathcal{N}+1}(x)\|_\omega^2 = \int_0^1 |f(x) - P_{\mathcal{N}+1}(x)|^2\, \omega(x) dx$$
$$= \int_0^1 \left|\frac{2\|f\|_\infty}{4^{\mathcal{N}+1}(\mathcal{N}+1)!}\right|^2 \omega(x) dx \le \left[\frac{2\|f\|_\infty}{(\mathcal{N}+1)!\,4^{\mathcal{N}+1}}\right]^2 \int_0^1 \omega(x) dx. \tag{15}$$

Now, we use the fact that $\int_0^1 \omega(x)dx = 1$. Now, it is sufficient to employ the square roots in (15). Thus we have proved our desired result. ∎

The combined collocation method

Now, the discretized equation (10) is solved by letting its related solution can be written in the form (12). To this end, the following set of collocation points are taken

$$x_p = \frac{p}{\mathcal{N}}, \quad p = 0, 1, \ldots, \mathcal{N}. \tag{16}$$

Besides, we need to find the matrix representation forms of the functions w^{n+1}, w_x^{n+1}, and w_{xx}^{n+1} as unknowns in (10).

After combining the relation (6) and (13), we may rewrite Eq. (12) in the matrix formulation as

$$\mathcal{V}_{n+1,\mathcal{N}}(x) = \boldsymbol{X}_{\mathcal{N}}(x)\, \boldsymbol{D}^t\, \boldsymbol{A}_{\mathcal{N}}^n. \tag{17}$$

By using the collocation points (16) and inserting them into the foregoing relation (17) to arrive at

$$\boldsymbol{V}_{n+1} = \boldsymbol{Z}\, \boldsymbol{D}^t\, \boldsymbol{A}_{\mathcal{N}}^n, \quad \boldsymbol{V}_{n+1} = \begin{pmatrix} \mathcal{V}_{n+1,\mathcal{N}}(x_0) \\ \mathcal{V}_{n+1,\mathcal{N}}(x_1) \\ \vdots \\ \mathcal{V}_{n+1,\mathcal{N}}(x_{\mathcal{N}}) \end{pmatrix}, \quad \boldsymbol{Z} = \begin{pmatrix} \boldsymbol{X}_{\mathcal{N}}(x_0) \\ \boldsymbol{X}_{\mathcal{N}}(x_1) \\ \vdots \\ \boldsymbol{X}_{\mathcal{N}}(x_{\mathcal{N}}) \end{pmatrix}. \tag{18}$$

By utilizing two relations (7) and (17), the first-order and second-order derivatives in (10) can be approximated in the matrix representations as

$$\begin{cases} w_x^{n+1} \approx \mathcal{V}^{(1)}_{n+1,\mathcal{N}}(x) = \boldsymbol{X}_{\mathcal{N}}(x)\,\boldsymbol{Q}^t\,\boldsymbol{D}^t\,\boldsymbol{A}^n_{\mathcal{N}}, \\ w_{xx}^{n+1} \approx \mathcal{V}^{(2)}_{n+1,\mathcal{N}}(x) = \boldsymbol{X}_{\mathcal{N}}(x)\,(\boldsymbol{Q}^t)^2\,\boldsymbol{D}^t\,\boldsymbol{A}^n_{\mathcal{N}}. \end{cases} \tag{19}$$

By placing the collocation points, we may similarly express these derivatives in (19) in the matrix representations as

$$\boldsymbol{V}^{(1)}_{n+1} = \boldsymbol{Z}\,\boldsymbol{Q}^t\,\boldsymbol{D}^t\,\boldsymbol{A}^n_{\mathcal{N}}, \qquad \boldsymbol{V}^{(1)}_{n+1} = \begin{pmatrix} \mathcal{V}^{(1)}_{n+1,\mathcal{N}}(x_0) \\ \mathcal{V}^{(1)}_{n+1,\mathcal{N}}(x_1) \\ \vdots \\ \mathcal{V}^{(1)}_{n+1,\mathcal{N}}(x_{\mathcal{N}}) \end{pmatrix}, \tag{20}$$

$$\boldsymbol{V}^{(2)}_{n+1} = \boldsymbol{Z}\,(\boldsymbol{Q}^t)^2\,\boldsymbol{D}^t\,\boldsymbol{A}^n_{\mathcal{N}}, \qquad \boldsymbol{V}^{(2)}_{n+1} = \begin{pmatrix} \mathcal{V}^{(2)}_{n+1,\mathcal{N}}(x_0) \\ \mathcal{V}^{(2)}_{n+1,\mathcal{N}}(x_1) \\ \vdots \\ \mathcal{V}^{(2)}_{n+1,\mathcal{N}}(x_{\mathcal{N}}) \end{pmatrix}. \tag{21}$$

We next introduce the following notations

$$k_0^n(x) = 2 + \alpha\,\delta t\,w_x^n + \beta\,\delta t(1 - 2w^n), \qquad k_1^n(x) = \alpha\,\delta t\,w^n,$$
$$k_2^n(x) = -\delta t\,\gamma, \qquad g^n(x) = (2 - \beta\,\delta t)w^n + \delta t\,\gamma\,w^n_{xx}.$$

Thus, by utilizing the approximations $\mathcal{V}_{n+1,\mathcal{N}}(x), \mathcal{V}^{(1)}_{n+1,\mathcal{N}}(x), \mathcal{V}^{(2)}_{n+1,\mathcal{N}}(x)$, we may rewrite (10) as

$$k_2^n(x)\,\mathcal{V}^{(2)}_{n+1,\mathcal{N}}(x) + k_1^n(x)\,\mathcal{V}^{(1)}_{n+1,\mathcal{N}}(x) + k_0^n(x)\,\mathcal{V}_{n+1,\mathcal{N}}(x) = g^n(x), \quad 0 \le x \le 1. \tag{22}$$

The set of collocation points (16) will now be inserted into (22) to obtain the following system of equations

$$\boldsymbol{K}_{n,2}\,\boldsymbol{V}^{(2)}_{n+1} + \boldsymbol{K}_{n,1}\,\boldsymbol{V}^{(1)}_{n+1} + \boldsymbol{K}_{n,0}\,\boldsymbol{V}_{n+1} = \boldsymbol{G}_n. \tag{23}$$

In (23), the vector $\boldsymbol{G}_n$ as well as the matrices $\boldsymbol{K}_{n,\ell}$ are given by

$$\boldsymbol{G}_n = \begin{pmatrix} g^n(x_0) \\ g^n(x_1) \\ \vdots \\ g^n(x_{\mathcal{N}}) \end{pmatrix}_{(\mathcal{N}+1)\times 1},$$

$$\boldsymbol{K}_{n,\ell} = \begin{pmatrix} k^n_\ell(x_0) & 0 & \dots & 0 \\ 0 & k^n_\ell(x_1) & \dots & 0 \\ \vdots & \vdots & \ddots & \vdots \\ 0 & 0 & \dots & k^n_\ell(x_{\mathcal{N}}) \end{pmatrix}_{(\mathcal{N}+1)\times(\mathcal{N}+1)},$$

for $\ell = 0, 1, 2$. We shall put the relations (18), (20)–(21) into (23). This yields the following fundamental matrix of linear equations

$$\boldsymbol{W}^n\,\boldsymbol{A}^n_{\mathcal{N}} = \boldsymbol{G}_n, \tag{24}$$

where

$$\boldsymbol{W}^n := \left\{\boldsymbol{K}_{n,2}\,\boldsymbol{Z}\,(\boldsymbol{Q}^t)^2 + \boldsymbol{K}_{n,1}\,\boldsymbol{Z}\,\boldsymbol{Q}^t + \boldsymbol{K}_{n,0}\,\boldsymbol{Z}\right\}\,\boldsymbol{D}^t.$$

The resultant matrix equation (24) consists of $(\mathcal{N}+1)$ equations and $(\mathcal{N}+1)$ unknown coefficients $a_0^n, a_1^n, \dots, a^n_{\mathcal{N}}$ to be found. To solve (24), any classical linear solver can be used.

To take boundary conditions (11) into consideration, we need to write them in a matrix form. Using the representation (17), the boundary conditions $\mathcal{V}_{n+1,\mathcal{N}}(0) = f_0^{n+1}$ and $\mathcal{V}_{n+1,\mathcal{N}}(1) = f_1^{n+1}$ are expressed in the matrix notations

$$\widehat{\boldsymbol{W}}^n_0\,\boldsymbol{A}^n_{\mathcal{N}} = f_0^{n+1}, \qquad \widehat{\boldsymbol{W}}^n_0 := \boldsymbol{X}_{\mathcal{N}}(0)\,\boldsymbol{D}^t = [\hat{w}^0_0 \quad \hat{w}^0_1 \quad \dots \quad \hat{w}^0_{\mathcal{N}}],$$
$$\widehat{\boldsymbol{W}}^n_1\,\boldsymbol{A}^n_{\mathcal{N}} = f_1^{n+1}, \qquad \widehat{\boldsymbol{W}}^n_1 := \boldsymbol{X}_{\mathcal{N}}(1)\,\boldsymbol{D}^t = [\hat{w}^1_0 \quad \hat{w}^1_1 \quad \dots \quad \hat{w}^1_{\mathcal{N}}].$$

To proceed, the two rows (first and last ones) of the matrix $[\boldsymbol{W}^n;\boldsymbol{G}_n]$ will be replaced by two vectors $[\widehat{\boldsymbol{W}}^n_0; f_0^{n+1}]$ and $[\widehat{\boldsymbol{W}}^n_1; f_1^{n+1}]$. As a consequence, we get a modified algebraic system of equations given as follows

$$\left[\widehat{\boldsymbol{W}}^n;\widehat{\boldsymbol{G}}_n\right] = \begin{pmatrix} \hat{w}^0_0 & \hat{w}^0_1 & \hat{w}^0_2 & \hat{w}^0_3 & \dots & \hat{w}^0_{\mathcal{N}} & ; & f_0^{n+1} \\ w^1_0 & w^1_1 & w^1_2 & w^1_3 & \dots & w^1_{\mathcal{N}} & ; & g^n(x_1) \\ w^2_0 & w^2_1 & w^2_2 & w^2_3 & \dots & w^2_{\mathcal{N}} & ; & g^n(x_2) \\ \vdots & \vdots & \vdots & \ddots & \vdots & \vdots & ; & \vdots \\ w^{N-1}_0 & w^{N-1}_1 & w^{N-1}_2 & w^{N-1}_3 & \dots & w^{N-1}_{\mathcal{N}} & ; & g^n(x_{N-1}) \\ \hat{w}^1_0 & \hat{w}^1_1 & \hat{w}^1_1 & \hat{w}^1_3 & \dots & \hat{w}^1_{\mathcal{N}} & ; & f_1^{n+1} \end{pmatrix}.$$

Consequently, we get the Boole coefficients in (17) after solving the former modified linear system.

Experimental results and discussions

To illustrate the utilities of the present combined Taylor and Boole spectral collocation strategy, we consider several test problems for the underlying nonlinear model problem (1)–(3). For comparison, we utilize the exact solution (Wazwaz, 2005)

$$w(x,t) = \frac{1}{2}\left(1 + \tanh\left(\frac{-\alpha\,x}{4\gamma} + \frac{\alpha^2 - 4\beta\gamma}{8\gamma}t\right)\right), \quad (x,t) \in [0,1]\times[0,T]. \tag{25}$$

From the given exact solution, we can extract the boundary and the initial conditions appropriately. We use MATLAB 2017a for numerical simulations. The numerical computations are done on a personal laptop with Intel(R) Core(TM) i7-4500U, CPU 1.8 GHz and RAM 8 GB.

To measure errors, we also compute the absolute error (AE) achieved at time frame t_n given by

$$e_n(x) := |w(x,t_n) - \mathcal{V}_{n,\mathcal{N}}(x)|, \quad n = 1, 2, \dots, \mathcal{M}. \tag{26}$$

We next compute the L_2 and L_∞ error norms calculated at time $t = T$ by

$$E_2 \equiv E_2^{\mathcal{M},\mathcal{N}} := \sqrt{\frac{1}{\mathcal{N}+1}\int_0^1 [w(x,T) - \mathcal{V}_{\mathcal{M},\mathcal{N}}(x)]^2 dx},$$
$$E_\infty \equiv E_\infty^{\mathcal{M},\mathcal{N}} := \max_{0\le x\le 1} |w(x,T) - \mathcal{V}_{\mathcal{M},\mathcal{N}}(x)| = \max_{0\le x\le 1} e_{\mathcal{M}}(x).$$

We calculate next the associated (numerical) order of convergence (Noc) for the L_∞ and L_2 error norms. In this respect, we set

$$\text{Noc}^x_* := \log_2 \frac{E_*^{\mathcal{M},\mathcal{N}}}{E_*^{\mathcal{M},2\mathcal{N}}}, \quad \text{Noc}^t_* := \log_2 \frac{E_*^{\mathcal{M},\mathcal{N}}}{E_*^{2\mathcal{M},\mathcal{N}}}, \quad * = 2, \infty. \tag{27}$$

In addition, for validation, comparisons with existing numerical models and experimental results have been done. In this respect, we utilize the B-spline collocation method (BSCM) (Singh et al., 2020), the finite element method (FEM) (Yadav and Jiwari, 2017), the non-standard finite difference scheme 1 (NFSD1) (Namjoo et al., 2018), the optimal homotopy asymptotic method (OHAM) (Nawaz et al., 2013), the exp-function method (EFM) (Malik et al., 2015), the compact finite difference method (CFDM) (Sari et al., 2010).

Test case 1. Let us first consider the Fisher equation (1) using the parameters $\alpha = 0, \beta = -6, \gamma = 1$ (Izadi and Srivastava, 2022). In this case, we have the exact true solution as

$$w(x,t) = (1 + exp(x - 5t))^{-2}.$$

We first employ $\delta t = 0.01$ and $T = 0.1$. Using (12) with $\mathcal{N} = 5$, the following approximative solutions at $t = \delta t$ and $t = T$ for $0 \le x \le 1$ are obtained

$$\mathcal{V}_{1,5}(x) = 0.00173187272\,x^5 - 0.01454481408\,x^4 + 0.02541816092\,x^3 + 0.05852162569\,x^2 - 0.2560036827\,x + 0.2626535814,$$

Table 1
Comparing the L_∞ and L_2 error norms in Test case 1 utilizing $\delta t = 0.001$, $T = 0.01, 0.1, 1$, and various $\mathcal{N}$.

$\mathcal{N}$	$T = 0.01$		$T = 0.1$		$T = 1$		M_1	ADE-FTLag(0) (Izadi and Srivastava, 2022)
	L_∞	L_2	L_∞	L_2	L_∞	L_2		L_2 ($T = 0.01$)
5	2.09_{-6}	1.39_{-08}	4.82_{-6}	4.08_{-7}	6.83_{-8}	2.00_{-8}	25	3.1773_{-4}
6	2.58_{-7}	1.56_{-09}	2.05_{-7}	1.63_{-9}	3.07_{-8}	8.03_{-9}	50	3.2354_{-4}
7	2.75_{-8}	1.33_{-10}	2.25_{-7}	1.75_{-9}	2.97_{-8}	7.79_{-9}	100	3.2444_{-4}
8	2.86_{-8}	4.69_{-11}	2.66_{-7}	7.50_{-9}	2.92_{-8}	6.76_{-9}	200	3.3735_{-4}

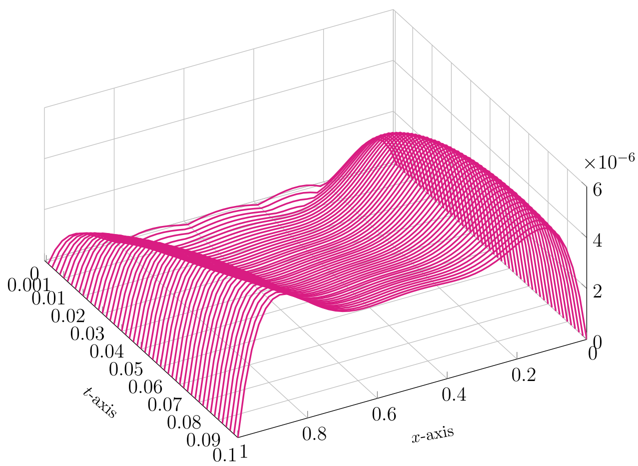

Fig. 1. The behavior of absolute errors for Test case 1 at diverse time snapshots $t = m\delta t, m = 1, 2 \ldots, 50$ (right) for $\delta t = 0.002$, $\mathcal{N} = 5$, and $T = 0.1$.

$$\mathcal{V}_{10,5}(x) = -0.002035235397\,x^5 - 0.005048494417\,x^4 + 0.03604705687\,x^3 + 0.01844932135\,x^2 - 0.2923313108\,x + 0.387455619.$$

A graphical picture of the obtained absolute errors is presented in Fig. 1. These errors are obtained via relation (26) at $x \in [0, 1]$ for $\delta t = 0.002$, $T = 0.1$ and various $t = m\delta t$, $m = 1, 2, \ldots, 50$. It should be stressed that we can get more accuracy in the results if we decrease δt or increase $\mathcal{N}$ in the computations appropriately.

For validation of our results, we do some comparisons presented in Table 1. Table 1 presents the errors acquired by the presented combined technique computed at times $T = 0.01, 0.1, 1$ and for $x \in [0, 1]$. We set the time step as $\delta t = 0.001$ in all computations. Also, the analogue results of a split-step finite difference scheme (Izadi and Srivastava, 2022) termed ADE-FTLag(0) (with M_1 as the number of spacial grid points) are reported in Table 1. Clearly, the results indicate the utility of the combined technique, which has less computational complexity and works better in terms of accuracy than the ADE-FTLag(0).

Test case 2. Let us now consider the Burgers–Fisher model equation with parameters $\alpha, \beta = -1$, and $\gamma = 1$. The exact solution is given via relation (25). This problem is previously considered in Singh et al. (2020), Yadav and Jiwari (2017).

We firstly employ $T = 0.1$, $\delta t = 0.01$, and $\mathcal{N} = 5$. By using these parameters, we acquire the approximated solutions at times $t = \delta t$ and $t = T$ as follow

$$\mathcal{V}_{1,5}(x) = 0.00005558870802\,x^5 + 0.00002143286985\,x^4 - 0.002610870576\,x^3 - 0.0001939231497\,x^2 + 0.1249951626\,x + 0.5031249593,$$

$$\mathcal{V}_{10,5}(x) = 0.00004728206701\,x^5 + 0.0001004836054\,x^4 - 0.002574715632\,x^3 - 0.001941275775\,x^2 + 0.124513717\,x + 0.5312093734.$$

Let us fix $\mathcal{N} = 5$ and vary δt to observe the behavior of achieved absolute errors. The visualizations of $e_1(t)$ at different time snapshots $t = T$, $T = 0.1, 0.1/2, 0.1/4, 0.1/8$ are shown in Fig. 2, left picture. We next see how the absolute errors are behaved when $\delta t = 0.001$, $T = \delta t$, are fixed and different $\mathcal{N} = 2, 4, 8$ are used. In this case, the results are depicted in Fig. 2, see right panel.

Table 2
The achieved error norms E_2 and E_∞ and their associated Noc in Test case 2 for fixed values $\mathcal{N} = 5, \delta t = 7.8125 \times 10^{-4}$, $T = 1$, and various $\delta t, \mathcal{N}$ for $x \in [0, 1]$.

δt	$\mathcal{N} = 5$				$\mathcal{N}$	$\delta t = 7.8125 \times 10^{-4}$			
	E_2	Noc_2^t	E_∞	Noc_∞^t		E_2	Noc_2^x	E_∞	Noc_∞^x
$\frac{1}{4}$	5.9118_{-5}	–	2.0212_{-4}	–	1	1.5215_{-3}	–	2.9481_{-3}	–
$\frac{1}{8}$	1.4718_{-5}	2.0060	4.9592_{-5}	2.0270	2	9.5154_{-6}	7.3210	2.8428_{-5}	6.6963
$\frac{1}{16}$	3.6770_{-6}	2.0010	1.2383_{-5}	2.0017	4	6.7377_{-8}	7.1419	2.6955_{-7}	6.7206
$\frac{1}{32}$	9.1795_{-7}	2.0020	3.0915_{-6}	2.0020	8	4.5361_{-10}	7.2147	1.9354_{-9}	7.1218

The second-order accuracy of the present method with regard to time and the higher-order accuracy in space variable will be shown in next experiments. Towards this end, we first fixed $\mathcal{N} = 5$ and vary $\delta t = 1/2^j$ for $j = 2, 3, 4, 5$. Then, we compute the numerical order of convergence in both L_2 and L_∞ norms via relations (27). The results for $T = 1$ are tabulated in Table 2. On the other hand, we fixed $\delta t = 7.8125{\times}10^{-4}$ while diverse values of $\mathcal{N} = 1, 2, 4, 8$ are utilized in the computations. By looking at the results presented in Table 2 one sees that the Noc_*^t equal to 2 and a higher-order accuracy for Noc_*^x about seven are obtained in the second Test case 2.

For comparison, results of the former existing available methods are shown in Table 3. Towards this end, we use the BSCM (Singh et al., 2020) and the FEM (Yadav and Jiwari, 2017) (with $\delta t = 10^{-5}$). Obviously, our numerical results with a larger time step are more accurate compared to other computational schemes.

Test case 3. Let us take the Burgers–Fisher equation with $\alpha = 0.001$, $\beta = -0.001$, and $\gamma = 1$. This problem was solved in Singh et al. (2020), Yadav and Jiwari (2017) and its exact solution is given by (25).

For this test case, let us consider a large step size $\delta t = 1$ and $T = 10$. Utilizing $\mathcal{N} = 5$, we arrive at the next approximations computed at the end-points $t = \delta t$ as well as $t = T$ respectively as

$$\mathcal{V}_{1,5}(x) = -1.032872 \times 10^{-16}\,x^5 - 2.801605 \times 10^{-12}\,x^4 + 8.205014 \times 10^{-12}\,x^3 - 3.635841773 \times 10^{-11}\,x^2 - 0.0001249999508\,x + 0.5002500625,$$

$$\mathcal{V}_{10,5}(x) = 2.763911 \times 10^{-16}\,x^5 + 5.24603 \times 10^{-12}\,x^4 - 7.890941 \times 10^{-12}\,x^3 - 1.601806 \times 10^{-10}\,x^2 - 0.0001249968643\,x + 0.5025006042.$$

The profile of numerical approximations for $\delta t = 0.2$, $T = 10$, and $\mathcal{N} = 5$ at diverse time snapshots $t = m\delta t$, $m = 1, 2, \ldots, 50$ are plotted in Fig. 3. The related exact true solutions are shown by thick lines. The difference between numerical and exact true solutions are also visualized in the left picture. Clearly as seen, an excellent alignment between our obtained numerical outcomes and the associated exact true solutions can be observed.

Some comparisons with six existing well-established computational schemes are investigated in Table 4. Here, we use the BSCM (Singh et al., 2020), the FEM (Yadav and Jiwari, 2017), the NFSD1 (Namjoo et al., 2018), the OHAM (Nawaz et al., 2013), the EFM (Malik et al., 2015), and the CFDM (Sari et al., 2010). It can be concluded that

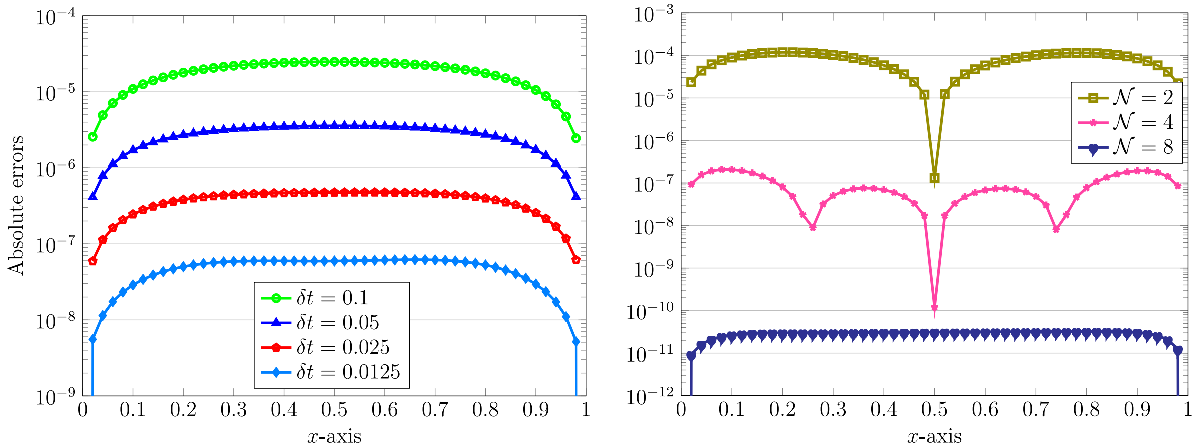

Fig. 2. The behavior of absolute errors utilizing $\mathcal{N} = 5$ (fixed), $T = 0.1/2^m$, $m = 0, 1, 2, 3$ (left) and $\delta t = 0.001$ (fixed), $T = \delta t$ (right) in Test case 2.

Table 3
Results of absolute errors for test case 2 with $\delta t = 0.001, 0.005, 0.01$, $T = \delta t$, $\mathcal{N} = 5$ and various $x \in [0, 1]$.

x	$T = 0.01$			$T = 0.005$			$T = 0.001$	
	Present	FEM (Yadav and Jiwari, 2017)	BSCM (Singh et al., 2020)	Present	FEM (Yadav and Jiwari, 2017)	BSCM (Singh et al., 2020)	Present	BSCM (Singh et al., 2020)
0.1	1.24_{-8}	4.99_{-7}	3.23_{-07}	2.92_{-9}	7.08_{-7}	4.66_{-07}	2.31_{-9}	1.70_{-08}
0.5	3.01_{-8}	1.08_{-6}	5.53_{-10}	2.94_{-9}	1.69_{-6}	1.09_{-13}	7.22_{-9}	2.53_{-14}
0.9	1.21_{-8}	3.54_{-7}	3.21_{-07}	4.22_{-9}	5.11_{-7}	5.75_{-07}	4.50_{-9}	1.70_{-08}

Table 4
The outcomes of absolute errors in Test case 3 with $\mathcal{N} = 5$, $\delta t = T$, $T = 0.001, 0.005, 0.01$, and diverse $x, t \in [0, 1]$.

x	$t = T$	Present	BSCM (Singh et al., 2020)	NFSD1 (Namjoo et al., 2018)	FEM (Yadav and Jiwari, 2017)	OHAM (Nawaz et al., 2013)	EFM (Malik et al., 2015)	CFDM (Sari et al., 2010)
0.1	0.001	0	4.64_{-11}	5.551_{-17}	1.21_{-09}	2.25_{-8}	1.97_{-8}	1.01_{-7}
	0.005	5.55_{-17}	5.85_{-10}	1.665_{-16}	1.69_{-09}	1.12_{-7}	1.97_{-8}	4.38_{-7}
	0.01	0	8.84_{-10}	2.220_{-16}	1.28_{-09}	2.25_{-7}	1.97_{-8}	7.53_{-7}
0.5	0.001	0	5.39_{-14}	5.551_{-17}	2.28_{-12}	4.58_{-8}	3.58_{-9}	1.04_{-7}
	0.005	5.55_{-17}	2.73_{-13}	5.551_{-17}	2.49_{-09}	2.29_{-7}	3.71_{-9}	5.21_{-7}
	0.01	5.55_{-17}	2.04_{-12}	1.110_{-16}	2.50_{-09}	4.58_{-7}	3.88_{-9}	1.04_{-6}
0.9	0.001	1.11_{-16}	4.64_{-11}	1.665_{-16}	1.20_{-10}	4.58_{-8}	1.80_{-8}	1.01_{-7}
	0.005	0	5.85_{-10}	1.110_{-16}	1.69_{-09}	2.29_{-7}	1.77_{-8}	4.38_{-7}
	0.01	0	8.84_{-10}	1.110_{-16}	1.28_{-09}	4.58_{-7}	1.74_{-8}	7.53_{-7}

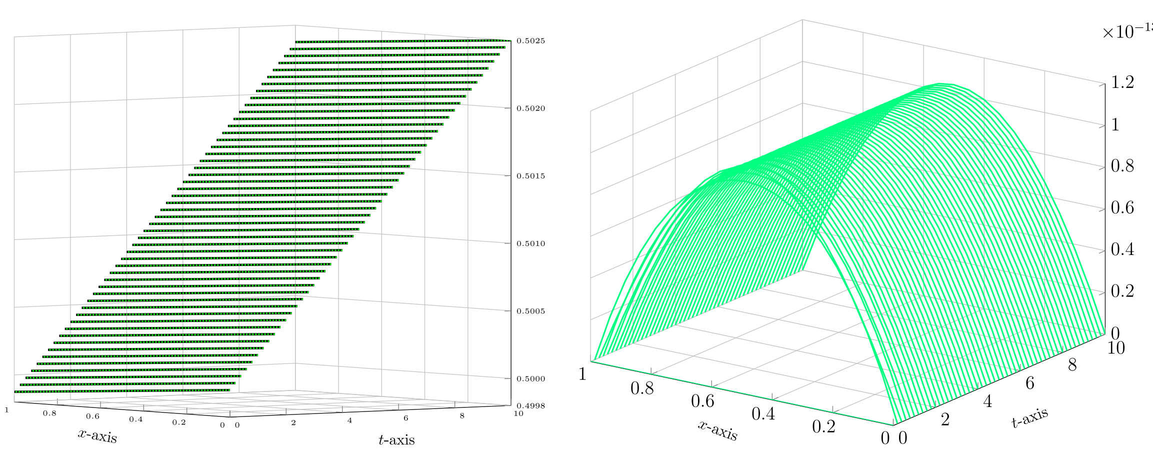

Fig. 3. Numerical/exact solutions (left) and the associated absolute errors in Test case 3 at diverse time snapshots $t = m\delta t, m = 1, 2, \ldots, 10$ (right) for $\delta t = 0.2, \mathcal{N} = 5$, and $T = 10$.

our proposed approach is superior in terms of accuracy using a lower number of basis functions. Furthermore, for long time computations, we calculate the L_∞ error norms with particularly a large time step $\delta t = 1$. The final times are taken as $T = 1, 5, 10, 50$, and $T = 100$. The outcomes are presented in Table 5. For each final time T, we use $\mathcal{N} = 2, 3, \ldots, 6$. We emphasize that the order of errors is the same for all values of T and even a decreasing function of T. This implies that the accuracy of present method is maintained over large time domains.

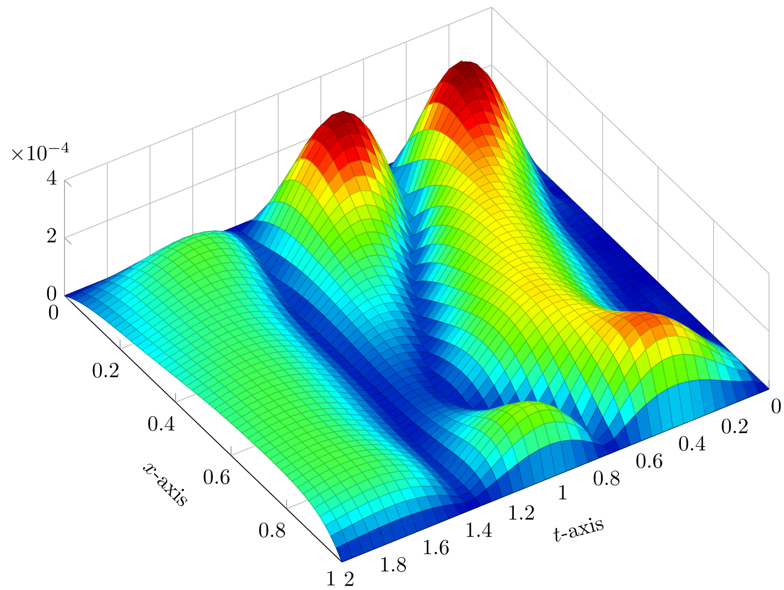

Fig. 4. Absolute errors for Burgers–Fisher equation using $\alpha = 1, \beta = -1, \gamma = 0.2$, for $\delta t = 0.05$, $T = 2$, and $\mathcal{N} = 5$.

Table 5
A comparison of L_∞ error norms in Test case 3 for various $\mathcal{N} = 2, 3, \ldots, 6$ and $\delta t = 1$ on large time intervals evaluated at $t = T$, with $T = 1, 5, 10, 50, 100$.

N	$T = 1$	$T = 5$	$T = 10$	$T = 50$	$T = 100$
2	4.1746_{-12}	2.8162_{-12}	2.5986_{-12}	2.6127_{-12}	2.6077_{-12}
3	4.2630_{-12}	2.8770_{-12}	2.5767_{-12}	2.6036_{-12}	2.5988_{-12}
4	4.3075_{-12}	2.8782_{-12}	2.6152_{-12}	2.6061_{-12}	2.5988_{-12}
5	4.3079_{-12}	2.8806_{-12}	2.6145_{-12}	2.6079_{-12}	2.5990_{-12}
6	4.3084_{-12}	2.8845_{-12}	2.6115_{-12}	2.6074_{-12}	2.5978_{-12}

In the next experiments, diverse values of $\alpha = 0.5$, $\beta = -0.5$, and $\alpha = 0.1$, $\beta = -0.1$ are used with $\gamma = 1$. For validation, we compare our numerical solutions with analytic HPM (Rashidi et al., 2009) as well as the BSCM (Singh et al., 2020). In Table 6, we report the absolute errors achieved via our presented procedure associated with $\delta t = 0.005$, $\mathcal{N} = 5$, $T = 0.1, 0.4, 0.8$, and some $x = 0.2, 0.4, 0.6, 0.8$. It can be noticed that our approach is more accurate than these methods.

We finally fix the parameters $\alpha = 0.01$ and $\gamma = 2$ and utilize diverse values of $\beta = -0.01, -0.1, -1, -10$ in the computations. In Table 7, we show the absolute errors computed at some points $x \in [0, 1]$ and obtained by using $\mathcal{N} = 3$, $\delta t = 0.01$. Also, different final times $T = 0.01, 0.5$, and $T = 1$ are utilized. Next, with $\mathcal{N} = 5$ and $\delta t = 0.005$, we fix $\beta = -1$, $\gamma = 0.1$ while α varies as $-0.01, -0.1, 0.01$ and 0.1. The result of absolute errors are tabulated in Table 8. In the last Table 9, we fix $\alpha = 0.001$ and $\beta = -1$ and use $\gamma = 0.001, 0.01, 0.1, 1$. In this case, $\mathcal{N} = 5$, $\delta t = 0.05$, and the final times $T = 0.1, 1, 2$ are used. Fig. 4 tabulates the absolute errors by setting $\mathcal{N} = 5$, $\delta t = 0.05$, and $T = 2$. The parameters used are $\alpha = 1$, $\beta = -1$, and $\gamma = 0.2$.

Conclusions

A simple and effective combined approximation algorithm have adapted to determine the solution of nonlinear Burgers–Fisher equation numerically. The well-known Taylor expansion approach was utilized for the time marching algorithm, which reduces the Burgers–Fisher model equation into a set of linearized initial boundary value problem (LIBVP). Afterwards, a matrix collocation procedure relied on the novel Boole functions was used to treat the resultant LIBVP in the space direction at each time level numerically. Based on the matrix formulation of these polynomials together with the given set of collocation nodes, the combined scheme transformed the LIBVP into a linear system of algebraic equations. The error and convergence analysis of the developed approach in the $\mathcal{L}_2$ norm were established. The utility as well as the accuracy of the proposed combined technique were examined by doing several numerical calculations. Comparisons with exact true solutions as well as with existing computational outcomes have also been carried out. The results shown in this work demonstrated the robustness of the combined approximation algorithm with less computational complexity for the nonlinear unsteady Burgers–Fisher equation.

Table 6
The comparison of absolute errors with $\mathcal{N} = 5$, $\delta t = 0.005$, $T = 0.1, 0.4, 0.8$, and various $x \in [0, 1]$.

T	x	$\alpha = -\beta = 0.1$			$\alpha = -\beta = 0.5$		
		Present	BSCM (Singh et al., 2020)	HPM (Rashidi et al., 2009)	Present	BSCM (Singh et al., 2020)	HPM (Rashidi et al., 2009)
0.1	0.2	2.7864_{-11}	2.1998_{-7}	4.3262_{-8}	3.9481_{-9}	1.2205_{-6}	6.1768_{-6}
	0.4	4.0017_{-11}	1.6726_{-7}	1.0883_{-7}	5.6624_{-9}	9.2477_{-7}	1.6029_{-5}
	0.6	4.0101_{-11}	1.6660_{-7}	1.7457_{-7}	5.7008_{-9}	9.0491_{-7}	2.5802_{-5}
	0.8	2.8051_{-11}	2.1871_{-7}	2.4012_{-7}	4.0496_{-9}	1.1797_{-6}	3.5447_{-5}
0.4	0.2	4.2253_{-11}	2.9985_{-7}	3.8516_{-7}	5.8867_{-9}	1.6342_{-6}	7.8774_{-5}
	0.4	6.3490_{-11}	2.9715_{-7}	6.6533_{-7}	9.0394_{-9}	1.6248_{-6}	7.8951_{-5}
	0.6	6.3696_{-11}	2.9713_{-7}	1.7158_{-6}	9.1863_{-9}	1.6277_{-6}	2.3628_{-4}
	0.8	4.2665_{-11}	2.9982_{-7}	2.7658_{-6}	6.1958_{-9}	1.6438_{-6}	3.9244_{-4}
0.8	0.2	4.3032_{-11}	3.0381_{-7}	7.2803_{-6}	5.8475_{-9}	1.6046_{-6}	1.2446_{-3}
	0.4	6.4769_{-11}	3.0384_{-7}	3.0801_{-6}	9.1633_{-9}	1.6189_{-6}	6.2245_{-4}
	0.6	6.4990_{-11}	3.0392_{-7}	1.1209_{-6}	9.3526_{-9}	1.6316_{-6}	2.8091_{-6}
	0.8	4.3473_{-11}	3.0403_{-7}	5.3215_{-6}	6.2393_{-9}	1.6427_{-6}	6.2804_{-4}

Table 7
The comparison of obtained absolute errors with $\mathcal{N}=3$, $\delta t=0.01$, $T=0.01,0.5,1$, fixed $\alpha=0.01$, $\gamma=2$, and various β.

x	T	$\beta=-0.01$	$\beta=-0.1$	$\beta=-1$	$\beta=-10$
0.1	0.01	7.7716_{-15}	7.7418_{-12}	7.7404_{-09}	7.7327_{-06}
	0.1	4.6962_{-14}	4.6835_{-11}	4.4051_{-09}	1.2449_{-06}
	1.0	4.7074_{-14}	4.6754_{-11}	3.6863_{-09}	8.5013_{-09}
0.4	0.01	2.14828_{-14}	2.1506_{-11}	2.1503_{-08}	2.1482_{-05}
	0.1	1.30451_{-13}	1.3014_{-10}	1.2242_{-07}	3.4616_{-06}
	1.0	1.30562_{-13}	1.2992_{-10}	1.0246_{-07}	2.3638_{-08}
0.9	0.01	7.7716_{-15}	7.7428_{-12}	7.7415_{-09}	7.7344_{-06}
	0.1	4.6962_{-14}	4.6868_{-11}	4.4095_{-08}	1.2474_{-06}
	1.0	4.6962_{-14}	4.6789_{-11}	3.6911_{-08}	8.5183_{-09}

Table 8
The comparison of achieved absolute errors with $\mathcal{N}=5$, $\delta t=0.005$, $T=0.01,0.1,1$, fixed $\beta=-1$, $\gamma=0.1$, and various α.

x	T	$\alpha=-0.01$	$\alpha=-0.1$	$\alpha=0.01$	$\alpha=0.1$
0.1	0.01	3.7223_{-09}	1.0559_{-09}	3.7219_{-09}	8.4632_{-09}
	0.1	3.2338_{-08}	2.4426_{-08}	3.2304_{-08}	3.8272_{-08}
	1.0	1.2411_{-07}	1.1864_{-07}	1.2392_{-07}	1.0522_{-07}
0.5	0.01	5.1037_{-09}	4.1504_{-09}	5.1048_{-09}	6.2094_{-09}
	0.1	5.1663_{-08}	5.2131_{-08}	5.1791_{-08}	5.3309_{-08}
	1.0	3.1116_{-07}	2.8189_{-07}	3.1843_{-07}	3.5718_{-07}
0.9	0.01	3.7192_{-09}	2.3410_{-09}	3.7213_{-09}	9.3098_{-09}
	0.1	3.2209_{-08}	1.9450_{-08}	3.2403_{-08}	3.9655_{-08}
	1.0	1.2105_{-07}	8.8883_{-08}	1.2697_{-07}	1.3817_{-07}

Table 9
The comparison of achieved absolute errors with $\mathcal{N}=5$, $\delta t=0.05$, $T=0.1,1,2$, fixed $\alpha=0.001$, $\beta=-1$, and various γ.

x	T	$\gamma=0.001$	$\gamma=0.01$	$\gamma=0.1$	$\gamma=1$
0.1	0.1	3.7883_{-06}	3.7137_{-06}	3.2398_{-06}	1.5754_{-06}
	1.0	2.9964_{-05}	2.5527_{-05}	1.2399_{-05}	1.8431_{-06}
	2.0	3.1873_{-05}	2.3988_{-05}	8.6512_{-06}	9.8422_{-07}
0.5	0.1	5.0656_{-06}	5.0982_{-06}	5.1681_{-06}	4.0574_{-06}
	1.0	4.4518_{-05}	4.1256_{-05}	3.1516_{-05}	5.1205_{-06}
	2.0	5.1664_{-05}	4.4225_{-05}	2.3482_{-05}	2.7344_{-06}
0.9	0.1	3.6782_{-06}	3.7198_{-06}	3.2409_{-06}	1.5755_{-06}
	1.0	3.4615_{-05}	2.6021_{-05}	1.2430_{-05}	1.8436_{-06}
	2.0	4.2308_{-05}	2.4757_{-05}	8.6807_{-06}	9.8455_{-07}

Declaration of competing interest

The authors declare that they have no known competing financial interests or personal relationships that could have appeared to influence the work reported in this paper.

Data availability

Data sharing not applicable to this article as no datasets were generated or analyzed during the current study.

References

Ahmed, H.M., 2019. Numerical solutions of Korteweg–de Vries and Korteweg–de Vries-Burger's equations in a Bernstein polynomial basis. Mediter. J. Math. 16, 102. http://dx.doi.org/10.1007/s00009-019-1375-1.

Ahmed, N., Elsonbaty, A., Raza, A., Rafiq, M., Adel, W., 2021. Numerical simulation and stability analysis of a novel reaction–diffusion COVID-19 model. Nonlinear Dyn. 106 (2), 1293–1310. http://dx.doi.org/10.1007/s11071-021-06623-9.

Bicer, K.E., Dag, H.G., 2023. Numerical solutions of differential equations having cubic nonlinearity using Boole collocation method. Turk. J. Math. 47, 732–745. http://dx.doi.org/10.55730/1300-0098.3391.

Bira, B., Mandal, H., Zeidan, D., 2019. Exact solution of the time fractional variant Boussinesq-Burgers equations. Appl. Math. 66, 437–449. http://dx.doi.org/10.21136/AM.2021.0269-19.

Chandrakera, V., Awasthib, A., Jayaraja, S., 2015. A numerical treatment of Fisher equation. Procedia Eng. 127, 1256–1262. http://dx.doi.org/10.1016/j.proeng.2015.11.481.

Doostaki, R., Hosseini, M.M., Salemi, A., 2023. A new simultaneously compact finite difference scheme for high-dimensional time-dependent PDEs. Math. Comput. Simul. 212, 504–523. http://dx.doi.org/10.1016/j.matcom.2023.05.008.

Izadi, M., 2020. Applications of the Newton–Raphson method in a SDFEM for inviscid Burgers equation. Comput. Methods Differ. Equ. 8 (4), 708–732. http://dx.doi.org/10.22034/cmde.2020.32615.1513.

Izadi, M., 2021. A second-order accurate finite-difference scheme for the classical Fisher-Kolmogorov-Petrovsky-Piscounov equation. J. Infor. Optim. Sci. 42 (2), 431–448. http://dx.doi.org/10.1080/02522667.2019.1696919.

Izadi, M., 2022. Two-stage explicit schemes based numerical approximations of convection–diffusion equations. Int. J. Comput. Sci. Math. 16 (3), 208–224. http://dx.doi.org/10.1504/IJCSM.2022.128185.

Izadi, M., Roul, P., 2023. A new approach based on shifted Vieta-Fibonacci-quasilinearization technique and its convergence analysis for nonlinear third-order Emden-Fowler equation with multi-singularity. Commun. Nonlinear Sci. Numer. Simul. 117, 106912. http://dx.doi.org/10.1016/j.cnsns.2022.106912.

Izadi, M., Srivastava, H.M., 2022. An optimized second order numerical scheme applied to the non-linear Fisher's reaction–diffusion equation. J. Interdiscip. Math. 25 (2), 471–492. http://dx.doi.org/10.1080/09720502.2021.1930662.

Izadi, M., Srivastava, H.M., 2023. Applications of modified Bessel polynomials to solve a nonlinear chaotic fractional-order system in the financial market: Domain-splitting collocation techniques. Computation 11 (7), 130. http://dx.doi.org/10.3390/computation11070130.

Izadi, M., Yüzbaşı, Ş., Cattani, C., 2023. Approximating solutions to fractional-order Bagley–Torvik equation via generalized Bessel polynomial on large domains. Ricerche Mat. 72 (1), 235–261. http://dx.doi.org/10.1007/s11587-021-00650-9.

Jiwari, R., 2015. A hybrid numerical scheme for the numerical solution of the Burgers' equation. Comput. Phys. Commun. 188, 59–67. http://dx.doi.org/10.1016/j.cpc.2014.11.004.

Jiwari, R., 2022. Local radial basis function-finite difference based algorithms for singularly perturbed Burgers' model. Math. Comput. Simul. 198, 106–126. http://dx.doi.org/10.1016/j.matcom.2022.02.024.

Jiwari, R., Gerisch, A., 2021. A local radial basis function differential quadrature semi-discretisation technique for the simulation of time-dependent reaction–diffusion problems. Eng. Comput. 38 (6), 2666–2691. http://dx.doi.org/10.1108/EC-05-2020-0291.

Jiwari, R., Kumar, S., Mittal, R.C., 2019. Meshfree algorithms based on radial basis functions for numerical simulation and to capture shocks behavior of Burgers' type problems. Eng. Comput. 36 (4), 1142–1168. http://dx.doi.org/10.1108/EC-04-2018-0189.

Jordan, C., 1950. Calculus of Finite Differences. Chelsea Publishing Company, New York.

Khader, M.M., Saad, K., 2018. A numerical approach for solving the fractional Fisher equation using Chebyshev spectral collocation method. Chaos Solit. Fract. 110, 169–177. http://dx.doi.org/10.1016/j.chaos.2018.03.018.

Kim, D.S., Kim, T., 2014. A note on Boole polynomials. Integ. Trans. Spec. Func. 25 (8), 627–633. http://dx.doi.org/10.1080/10652469.2014.891586.

Malik, S.A., Qureshi, I.M., Amir, M., Malik, A.N., Haq, I., 2015. Numerical solution to generalized Burgers-Fisher equation using exp-function method hybridized with heuristic computation. PLoS One 10, e0121728. http://dx.doi.org/10.1371/journal.pone.0121728.

Namjoo, M., Zeinadini, M., Zibaei, S., 2018. Nonstandard finite-difference scheme to approximate the generalized Burgers-Fisher equation. Math. Methods Appl. Sci. 41 (17), 8212–8228. http://dx.doi.org/10.1002/mma.5283.

Nawaz, R., Ullah, H., Islam, S., Idrees, M., 2013. Application of optimal homotopy asymptotic method to Burger equations. J. Appl. Math. 2013, 1–8. http://dx.doi.org/10.1155/2013/387478.

Negero, N.T., Duressa, G.F., 2022. Parameter-uniform robust scheme for singularly perturbed parabolic convection–diffusion problems with large time-lag. Comput. Methods Differ. Equ. 10 (4), 954–968. http://dx.doi.org/10.22034/cmde.2022.47907.2006.

Okhovati, N., Izadi, M., 2020. A predictor–corrector scheme for conservation equations with discontinuous coefficients. J. Math. Fund. Sci. 52 (3), 312–327. http://dx.doi.org/10.5614/j.math.fund.sci.2020.52.3.6.

Rashidi, M.M., Ganji, D.D., Dinarvand, S., 2009. Explicit analytical solutions of the generalized Burger and Burger-Fisher equations by homotopy perturbation method. Numer. Methods Partial Differ. Equ. 25, 409–417. http://dx.doi.org/10.1002/num.20350.

Razavi, M., Hosseini, M.M., Salemi, A., 2022. Error analysis and Kronecker implementation of Chebyshev spectral collocation method for solving linear PDEs. Comput. Methods Differ. Equ. 10 (4), 914–927. http://dx.doi.org/10.22034/cmde.2021.46776.1966.

Roman, S., 1984. The Umbral Calculus. New York.

Roul, P., Rohil, V., 2022. A high order numerical technique and its analysis for nonlinear generalized Fisher's equation. J. Comput. Appl. Math. 406, 114047. http://dx.doi.org/10.1016/j.cam.2021.114047.

Sabermahani, S., Ordokhani, Y., Hassani, H., 2021. General Lagrange scaling functions: application in general model of variable order fractional partial differential equations. Comput. Appl. Math. 40 (8), 269. http://dx.doi.org/10.1007/s40314-021-01667-4.

Sari, M., Gürarslan, G., Dag, I., 2010. A compact finite difference method for the solution of the generalized Burgers-Fisher equation. Numer. Methods Partial Differ. Equ. 26, 125–134. http://dx.doi.org/10.1002/num.20421.

Simsek, Y., So, J.S., 2019. Identities, inequalities for Boole-type polynomials: approach to generating functions and infinite series. J. Inequal. Appl. 2019, 62. http://dx.doi.org/10.1186/s13660-019-2006-x.

Singh, A., Dahiya, S., Singh, S.P., 2020. A fourth-order B-spline collocation method for nonlinear Burgers-Fisher equation. Math. Sci. 14, 75–85. http://dx.doi.org/10.1007/s40096-019-00317-5.

Srivastava, H.M., Izadi, M., 2022. The Rothe-Newton approach to simulate the variable coefficient convection–diffusion equations. J. Mahani Math. Res. 11 (2), 141–157. http://dx.doi.org/10.22103/jmmrc.2022.19497.1264.

Srivastava, H.M., Izadi, M., 2023. Generalized shifted airfoil polynomials of the second kind to solve a class of singular electrohydrodynamic fluid model of fractional order. Fractal Fract. 7 (1), 7. http://dx.doi.org/10.3390/fractalfract7010094.

Srivastava, V.K., Mishra, N., Kumar, S., Singh, B.K., Awasthi, M.K., 2014. Reduced differential transform method for solving $(1+n)$-dimensional Burgers' equation. Egyp. J. Basic Appl. Sci. 1 (2), 115–119. http://dx.doi.org/10.1016/j.ejbas.2014.05.001.

Stewart, G.W., 1996. Afternotes on Numerical Analysis, Vol. 49. SIAM.

Wazwaz, A.M., 2005. The tanh method for generalized forms of nonlinear heat conduction and Burgers-Fisher equations. Appl. Math. Comput. 169, 321–338. http://dx.doi.org/10.1016/j.amc.2004.09.054.

Yadav, O.P., Jiwari, R., 2017. Finite element analysis and approximation of Burgers-Fisher equation. Numer. Methods Partial Differ. Equ. 33 (5), 1652–1677. http://dx.doi.org/10.1002/num.22158.

Yang, X.-J., Gao, F., Srivastava, H.M., 2017. Exact travelling wave equations for the local fractional two-dimensional Burgers-type equations. Comput. Math. Appl. 73, 203–210. http://dx.doi.org/10.1016/j.camwa.2016.11.012.

Youssri, Y.H., Hafez, R.M., 2019. Exponential Jacobi spectral method for hyperbolic partial differential equations. Math. Sci. 13 (4), 347–354. http://dx.doi.org/10.1007/s40096-019-00304-w.

Zhang, R., Yu, X., Zhao, G., 2012. The local discontinuous Galerkin method for Burger's-Huxley and Burger's-Fisher equations. Appl. Math. Comput. 218, 8773–8778. http://dx.doi.org/10.1016/j.amc.2012.02.035.

Zhang, C., Zhang, Z., 2017. Application of the enhanced modified simple equation method for Burger-Fisher and modified Volterra equations. Adv. Differential Equations 2017, 145. http://dx.doi.org/10.1186/s13662-017-1198-y.